



## "Zn-Cr-LDH"-based Nano-Hybrids assembling at the presence of anions to Sense gas

Anil Kumar<sup>1</sup>, Amit Kumar Rawat<sup>2</sup>, Lata Vodwal<sup>3</sup>, Kamal Kant Tiwari<sup>4</sup>,  
Chandra Mohan<sup>5\*</sup>

<sup>1</sup>Assistant Professor, Deptt. of Physics, Bharati Vidyapeeth's College of Engineering, New Delhi 110063, India

<sup>2</sup>Assistant Professor, Deptt. of Chemistry, Hansraj College, New Delhi 110007, India

<sup>3</sup>Assistant Professor, Deptt. of Chemistry, Maitreyi College, New Delhi 110021, India

<sup>4</sup>Assistant Professor, Deptt. of Chemistry, National Institute of Technology, Srinagar 24617, India

<sup>5,\*</sup>Assistant Professor, Department of Chemistry, SBAS, K R Mangalam University, Gurugram-122103, India

\*Author for correspondence E-mail: [gurgaonmohan@yahoo.co.in](mailto:gurgaonmohan@yahoo.co.in)

---

### Abstract

In addition to traditional pollutant gases like CO and NH<sub>3</sub>, new ones like H<sub>2</sub>S, CO, NH<sub>3</sub>, NO<sub>2</sub>, CH<sub>4</sub>, and H<sub>2</sub> are becoming major factors in air pollution. In addition to facilitating a potentially disastrous barometric deviation, these gases also contribute to environmental changes and human development. Because of this, there has been a pressing need for the creation and deployment of a device for the fast confirmation of unambiguous ignitable, unstable, and poisonous gases. Semiconductor-based resistive gas sensors have risen in popularity due to their fast development in recent years. Sheared "Zn-Cr-LDH" nanosheets will therefore be joined together in a grid arrangement to generate nanohybrids as part of the continuing endeavour. The generated nanohybrids based on "Zn-Cr-LDH" are functional.

**Keywords:** "Zn-Cr-LDH"-based nanohybrids, Technology development, Gas sensors

---

### INTRODUCTION

Pollutants in the air have expanded all across the planet as a result of rapid urbanization, industrialization, and technological innovation. Successfully executed catastrophic floods due to autos and current endeavors create air defilement, one of the most obvious results. Human nature is profoundly affected by the air they breathe. Cl<sub>2</sub>'s greenish-yellow colour and genuinely strong fragrance make it ideal for use in insect sprays, insecticides, dark paper pound, materials, and pharmaceutical research. In addition, Cl<sub>2</sub> is used as a disinfectant in water treatment and sewage facilities. Cl<sub>2</sub> gas has various potential applications, but its most fundamental usage is to motivate people to work harder by making their tasks unpleasant or dangerous [1]. When exposed to high levels of Cl<sub>2</sub>, breathing may become difficult. Taking even a few deep breaths of Cl<sub>2</sub> may be fatal (concentration more than 1000 ppm). A weakening central structure is unconnected to stress, sickness, coughing, or chest discomfort. The addition of Cl<sub>2</sub> centre to flood water is a hazard to the land and water skilled climate in addition to being a threat to human growth. In the same vein, it plays a vital role as a direct component of the ozone layer [2].

Sulfur dioxide is a highly toxic, incapacitating, irritating, and opacity-reducing gas that is transported as a result of volcanic eruptions, incorrect waste disposal, and the burning

of petroleum wastes. The skin and eyes get irritated, the lungs become irritated, the waste is ejected down the neck, and there is a chance of death if SO<sub>2</sub> is inhaled. Fearsome winds aren't the only threat, however. In terms of SO<sub>2</sub> gas, the critical duration is 2 ppm, and the continuous second limit is 5 ppm. For this reason, researchers are working on extremely selective, very sensitive, and impressively generous gas sensors for Cl<sub>2</sub> and SO<sub>2</sub>. The semiconductor metal oxide sensors based on TiO<sub>2</sub>, SnO<sub>2</sub>, LaFeO<sub>3</sub>, and NiO are now the most widely available kind of gas sensor. However, these sensors need work at high temperatures to provide the best possible care and the quickest possible response. The high working temperature of the sensor makes it unsuitable for use in flammable or unpredictably hot settings. Researchers are constantly adjusting novel microstructure, ideal chemical design, jewel structure, pore improvement, and surface placement to build gas sensor materials that can work at low temperatures, therefore overcoming these obstacles [3,4].

Given these obstacles, research into mild LDHs is being conducted in order to develop gas sensors with exceptional sensing capability at ambient temperatures. LDHs are a family of cationic lamellar materials that have shown significant promise in a wide variety of applications over the past few decades, including electrochemistry, supports, drug enhancement materials, adsorbents for wastewater treatment, inspirations for combination corrosion, gas sensors, etc. Interlayer space between two regular LDH nanosheet is filled by water molecules and anions. LDH's layers offer ridiculously creative hiding spots for wandering atoms and molecules, including a habitat for hydrogen bonds and anions. Also, LDH has a shedding limit that gives a significant boost to guest moieties that intercalate and have clear roles to play. As a consequence, the hybridization process may affect the LDHs' optical, synergistic, and perceptual characteristics [5].

## **LITERATURE REVIEW**

According to Yang et al., 2019, Global warming is exacerbated by rising CO<sub>2</sub> levels in the atmosphere, hence efforts to capture and store the gas have been in high demand. The prospective uses of layered double hydroxides (LDHs) as CO<sub>2</sub> adsorbents and photocatalysts have drawn growing study attention. LDHs are also known as hydrotalcite-like compounds or ionic lamellar compounds.

Previous works have assessed the progress made with LDH-based materials employed as CO<sub>2</sub> adsorbents and photocatalysts independently. Rarely discussed in these synthesis and modification tactics of LDHs to increase adsorption capacities and photoreduction efficiencies for CO<sub>2</sub>. To that end, we've summed up key developments in this area that have occurred recently in this review. For direct fabrication of the necessary LDHs, the co-precipitation approach provides a quick and easy option that may be easily scaled up for mass production in an industrial setting. Doping LDHs with alkali metal, controlling particle properties, and fabricating connections are only some of the ways in which LDHs have been altered. The literature review here shows that modified LDH-based materials have shown promising results in the adsorption and photoreduction of CO<sub>2</sub>. Problems that still need fixing and ways in which LDHs might be enhanced are also mentioned [6].

Because of its malleable modular structure, easy exchangeability of inter-lamellar guest anions, and uniform distribution of metal cations throughout the layer, layered double hydroxides (LDHs) are an important big class of two-dimensional (2D) anionic lamellar materials. Polyoxometalates (POMs) intercalated with LDHs have shown a wide range of physical characteristics with applications in fields such as environment, energy, catalysis, etc., as a result of the modular accessible gallery and unique inter-lamellar chemical environment. In this article, we detail the creation of systems with essential catalytic capabilities using polyoxometalate clusters as building components. In this overview, we will mostly highlight recent advances in synthetic methods that make it possible to include design

into the creation of an entirely new category of materials with precisely specified properties for use in catalytic applications. Our work demonstrates the one-of-a-kind possibility of creating materials with modular characteristics for targeted catalytic applications by introducing the element of design and exercising control over the ultimately observed functionality [7].

De-NO<sub>x</sub> photocatalyst research was conducted on ZnAl-CO<sub>3</sub>, ZnAlCr-CO<sub>3</sub>, and ZnCr-CO<sub>3</sub> LDH samples. Pure LDH phase was used in the preparation of Cr-free samples and increasing Cr<sup>3+</sup> presence in the LDH framework at Cr/Zn ratios of 0.06, 0.15, and 0.3 using the co-precipitation technique. Chromium enrichment of the LDH framework reduces crystallinity and enhances specific surface area of the samples. Additionally, the CrO<sub>6</sub> octahedron centres broaden the photo-activity from UV to Visible light and help to reduce the recombination rate of electrons and holes. The excellent NO removal efficiency (55%) and remarkable selectivity (90%) reported for the analysed De-NO<sub>x</sub> process may be attributed to the Cr-containing LDH samples' favourable textural, optical, and electronic features [8].

"Anion clays, such as layered double hydroxides (LDHs) made up of brucite-like host layers and interlayer anions, are gaining popularity for use in the catalysis and adsorption fields. LDHs show great promise in the design and fabrication of nanomaterials used in photocatalysis, heterogeneous catalysis, and adsorption/separation processes due to their versatility in composition, morphology, and architecture, as well as their unique structural properties (intercalation, topological transformation, and self-assembly with other functional materials). The active centre structure (e.g., crystal facets, defects, geometric and electronic states, etc.) and macro-nano morphology of LDHs can be easily manipulated to achieve specific catalytic/adsorbent processes with greatly improved performances by taking advantage of the structural merits and various control synthesis strategies of LDHs. This article summarises recent developments in the design and preparation of LDH-based functional nanomaterials for long-term growth in catalysis and adsorption" [9].

## **MATERIALS AND METHODS**

Using a Rigaku miniflex 600 outfitted with Ni limited Cu k<sub>1</sub> cosmic rays (= 0.15406 nm), running at 30 kV with a destruction rate of 1 bachelor's, X-ray diffraction study of the valuable palisade wall of "Zn-Cr-LDH" was carried out. FE-SEM analysis was used to look at the morphology of LDH on Zn-Cr surfaces (Hitachi S-4800). In order to determine whether or not the compounds of interest were present in the metals, we used the T Food to do an iterative FT IR spectral analysis, narrowing in on a particular region of the spectrum between 400 and 4000 cm<sup>-1</sup>. Using Rg, a stunning investigation of the "Zn-Cr-LDH" meeting capability was conducted (Thermo Sensible DXR with 532 nm laser with excitation energy of 5mW power). Gas sorption scanning was used to preserve the microporous structure, pore curriculum, and interface location of Zn-Cr-unambiguous LDH by breaking down the Nitrogen adsorption - desorption framework at 77 K. (BELSORP bound scope II, Japan). The "Zn-Cr-LDH" has been degreased at 150 °C in a setting of 103 Torr for 4 hours in order to assess the N<sub>2</sub> thermodynamic characteristics. Electron imaging of the X-shaft was used to conduct a thorough examination of the positive charges of individual components.

## **RESULTS AND DISCUSSION**

### **X-Ray differaction study**

Understanding the "Zn-Cr-LDH" crystal structure requires X-ray diffraction investigation. The ""Zn-Cr-LDH"" is shown in Figure 1. Pure ""Zn-Cr-LDH"" exhibits highly developed (001) Constructive interference reflections, which reveal the presence of graphitic trigonal.

In order to determine the constants "a =0.308 nm and c =0.89" nm, a least-squares fitting analysis is performed, with the phases of "Zn-Cr-LDH" with NO<sub>3</sub> intercalation serving as the independent variable. Strong and sharp (00l) Bragg's reflections indicate that "Zn-Cr-LDH" likely possesses a hydrotalcite layered structure. Thus, the octahedral crystal structure in the XRD pattern confirms the "Zn-Cr-LDH" synthesis.

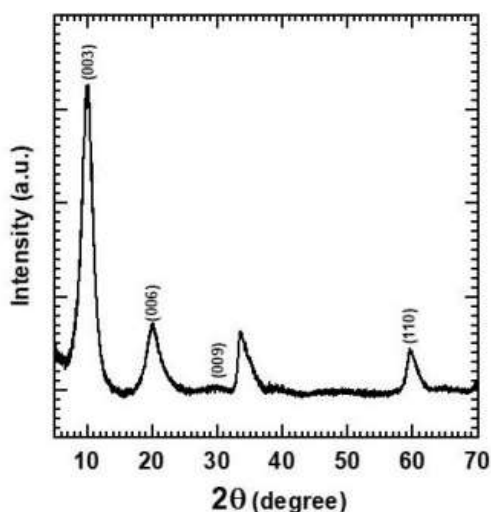


Figure 1. XRD pattern of "Zn-Cr-LDH".

### FT-IR study

The FT-IR spectroscopic study of a holding nature is shown in Figure 2. The asymmetrical widening process for intergallery nitrate anions, the bending vibrational processes for surrounding fluid, and the expanding oscillation of O-H social occasions are all linked with novel absorption peaks in "Zn-Cr-LDH" at 1384, 1615, and around 3400 cm<sup>-1</sup>. Perfect "Zn-Cr-LDH" has sharp support peaks at frequencies below 1000 cm<sup>-1</sup>, which are caused by the underlying iron vibrations. The growth of Zn Cr-LDH and nitrate ion intercalation have been monitored using the cutting-edge FT-IR laboratory.

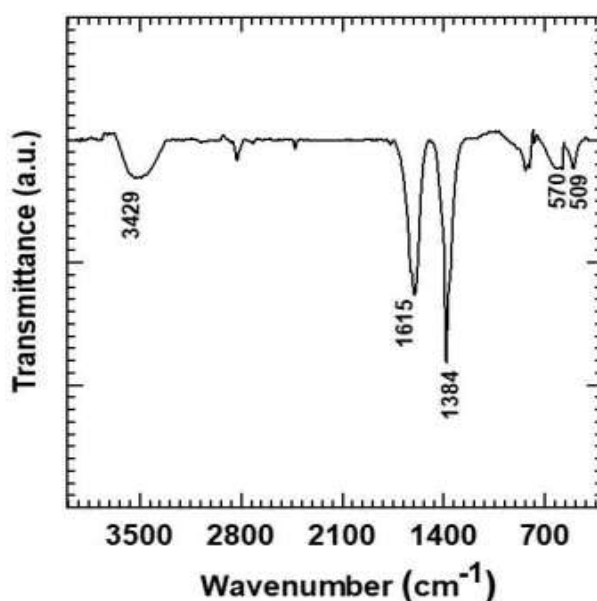


Figure 2. FT-IR spectrum of "Zn-Cr-LDH"

### Micro-Raman study

Phase change, stored combinations, and material type may all be assessed by infrared spectroscopy, which is a non-destructive technique. Figure 3 carefully monitors ZnCrLDH's minute Raman signature. Surprisingly, despite "Zn-Cr-LDH's" typically considerably lower Raman extent, it exhibits v1 to 5 expert Raman tops that are in agreement with the FTIR shifts of "Zn-Cr-LDH," intergallery ammonium ammonium ions, and H<sub>2</sub>O molecules. Furthermore, the interlayer NO<sub>3</sub><sup>-</sup> anions' asymmetrical development and out-of-plane perversion yields two enormous Raman peaks at 4 (719 cm<sup>-1</sup>) and 5. (1052 cm<sup>-1</sup>). A weakening of the Raman signal was found to be accompanied with an increase in Zn Cr-LDH and an intercalation of nitrate anion.

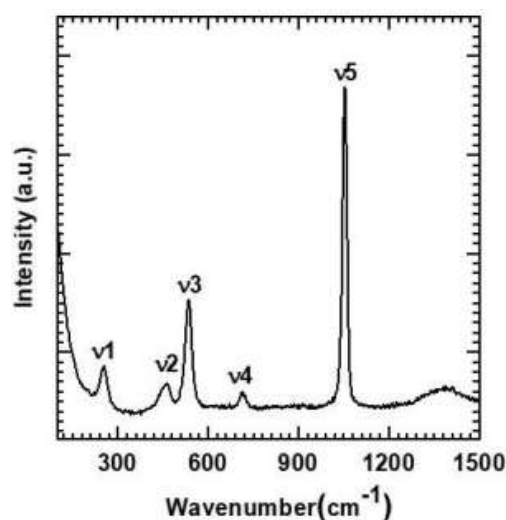


Figure 3. Micro-Raman spectrum of "Zn-Cr-LDH".

### FE-SEM study

To learn more about the morphological features of pure "Zn-Cr-LDH," we performed the FE-SEM study shown in Figure 4. Pure "Zn-Cr-LDH" consists of polymeric, densely packed particles of varying sizes. Particle sizes vary widely, from around 50 to 500 nm.

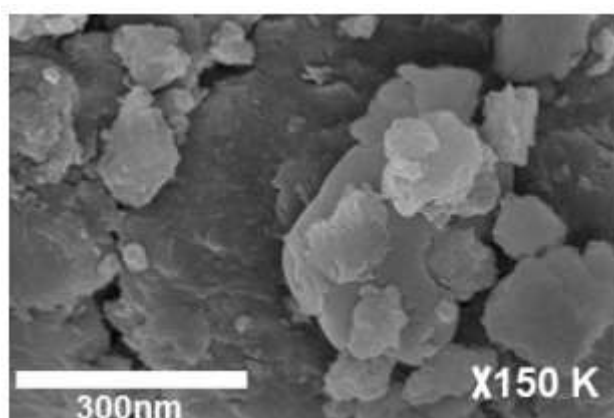


Figure 4. FE-SEM micrograph of "Zn-Cr-LDH".

### N<sub>2</sub> adsorption-desorption (BET) study

Figure 5 shows the results of a N<sub>2</sub> isotherm analysis of the water content and macroporous structure of pure "Zn-Cr-LDH."

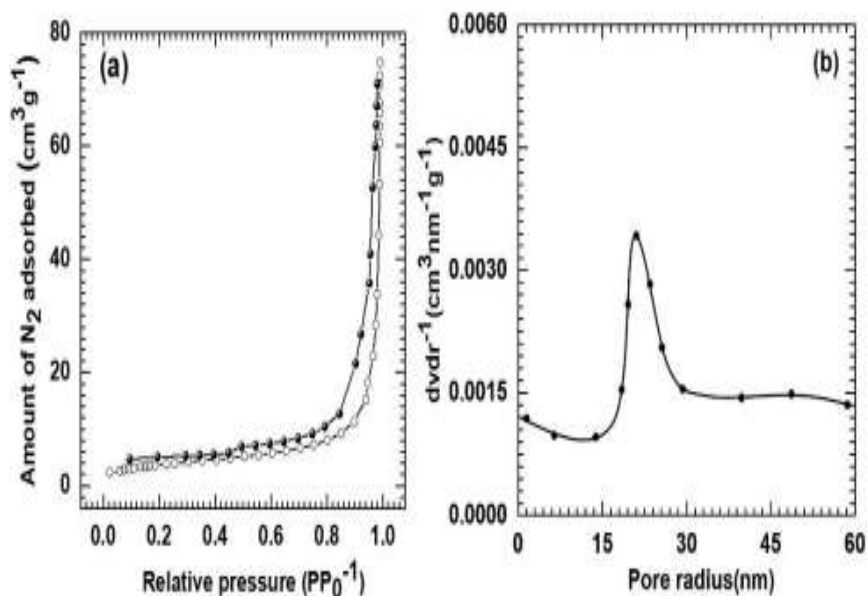


Figure 5. "(a) N<sub>2</sub> adsorption-desorption isotherm and (b) Pore size distribution curve of "Zn-Cr-LDH".

The mysterious "Zn-Cr-LDH" exhibited no N<sub>2</sub> binding at a ppo of 10.4, pointing to a limited surface area and a transparent or translucent structure. The adsorbate equations for Zn(III)Cr(IV)N<sub>2</sub>(aq)LDH are a Scherrer formula (BDDT) class formula with an extremely tiny persistence characteristic, as stated in the Special Relativity of Primary and Applied Mathematics (IUPAC). Zn-Cr has adapted brilliantly to the BET basis, however it is yet unclear what kind of surface area it is capable of producing. For such a geographical area, the ideal "Zn-Cr-LDH" has a tip of 12 m<sup>2</sup>g<sup>-1</sup>. Applying the Freeman (BJH) approach reveals a shift in the dispersion point of the Zn-Cr pore size distribution. The "Zn-Cr-LDH" body shown in Figure 5 has an average size much larger than 40 nm (b). According to the Bg assessment, "Zn-Cr-LDH" is a moderately hydrophobic compound.

### XPS study

The XPS was used to determine the components present, the fabrication states of those elements, and the "crystal structures of Zn-Cr-LDH." Store brand indicators at Zn, Cr, and O limiting frequencies determined by prepared samples of "Zn-Cr-LDH" are shown in Figure 6. (a). " At the P (1021.8eV), Q (1045 eV), R (577.8eV), and S (587.5eV) restriction energies, the Zn 2p<sub>3/2</sub>, Zn 2p<sub>1/2</sub>, Cr 2p<sub>3/2</sub>, and Cr 2p<sub>1/2</sub>, alone, stand out as conspicuous tops in Figure 6 (b) and (c). The primary maximum in the O 1s spectra from perfect "Zn-Cr-LDH" is shown in Figure 7(d), and it is attributable to air from the hydroxy group in the solid layer (because this maximum is limited to an energy of 531.3 eV).

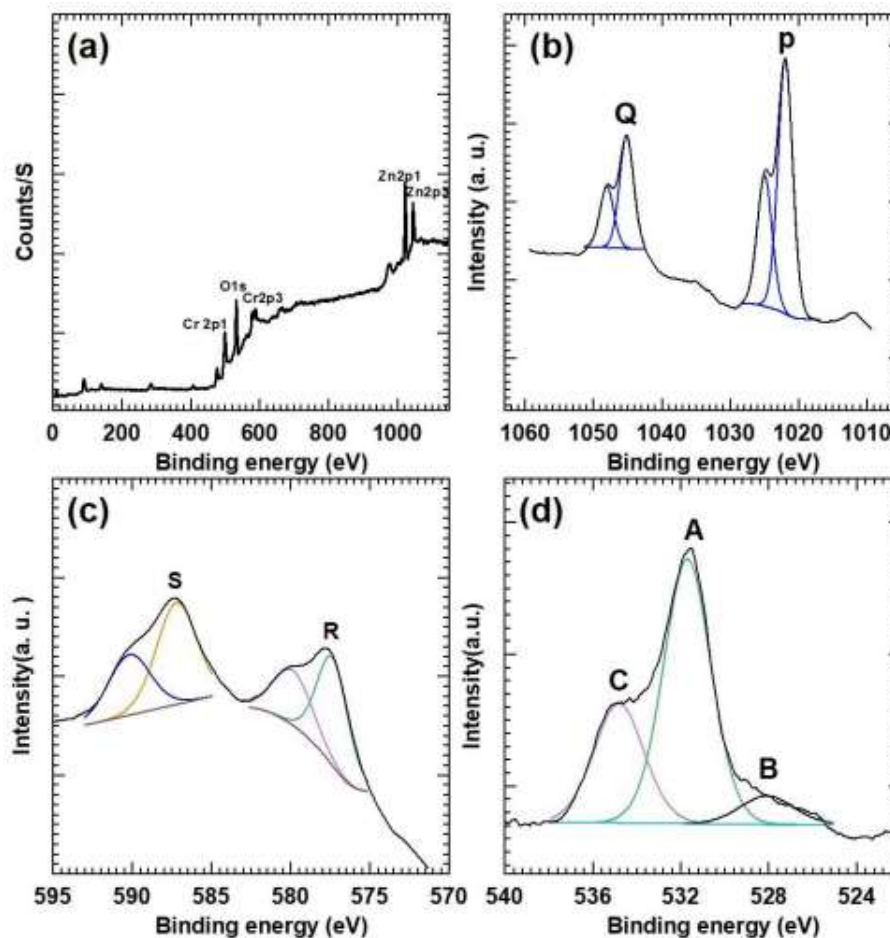


Figure 6. “(a) Survey, (b) Zn 2p, (c) Cr 2p, and (d) O 1s core-level XPS spectra of ZnCr-LDH”.

### Experimental Setup for gas sensor studies

Using a gas perceptive assessment framework, we tested pure Zn Cr-LDH in a series of gas reactions. The gas chamber is constructed from high-quality, shut-treated steel, and the gas got volume is no more than 315 cm<sup>3</sup>. The gas sound and outlet diagram, the warming turn got, and the configurable tests round out the gas seeing design. In order to keep track of the resistance response to actual gas entry and exit, the sensor component must be connected outside to a receiving structure. Each and every experiment designed to measure responses was carried out. The sensor component was fastened in the gas chamber's hermetically sealed, waterproof, and airtight enclosing holder by use of the holder's two helpful contact primers. The sensor part was tested by making connections at each end using silver paste and a corresponding gold push contact. Sensor responses to several test gases were evaluated using just one square centimeter of the satellite's surface area.

In order to determine the present stage of sensor development, a thermo controller was used to warm the supplied sensor component to the assessed working temperature for 30 minutes. Meanwhile, the gas chamber was shut up effectively once the sensor component was swapped out. In the end, the change in isolating section block was documented using a PC-controlled Keithley 6514 electrometer. Once a reliable deterrent regard had been obtained, the gas chamber was fine-tuned with comparable air to maintain initial sensor check. Reaction time refers to the test gas when the sensor's air confidence (Ra) and gas confidence (Rg) may be accepted at face value. Eq. does not fully resolve the selectivity (K) of the impedance throughout the target gas (1),

$$K = \frac{S(\text{Target gas})}{S(\text{Interference gas})}$$

The transmitter readings for the aim and distraction gases are denoted by S(Target gas) as well as S(interference gas), resp.

### Sensor element fabrication

Zn-Cr-LDH and other biosensors were delivered to the gas substrate using an expert jurisdictional approach. For 10 minutes, labogent chemical, water, (CH<sub>3</sub>)<sub>2</sub>CO, vodka, and water were used in sonic showers to clean the doped. Coated glass samples were washed and handled by water before being utilized. A combination of "Zn-Cr-LDH" recognizing material, polyvinylpyrrolidone, and - pinene with a gravity heavy of part of 80:15:5 was ground until it changed into homogeneous slurry of the promised thickness in order to manufacture the numerous sensor components. Furthermore, a thick covering of the resultant homogeneous slurry was regularly seen on well cleaned beakers (10 mm x 10 mm). To improve stability and mitigate the limiting influence of the limiting medium (polyvinyl alcohol), components of the "Zn-Cr-LDH" sensor were stimulated at 150 °C for 2 hours during production.

Table 1: Variation of the response and recovery characteristics of Zn-Cr LDH with different concentrations of Cl<sub>2</sub> and SO<sub>2</sub> at RT (27±2 °C).

Sample	Concentrations of (Cl <sub>2</sub> and SO <sub>2</sub> ) gas in ppm	Response time (s)		Recovery time (s)	
		Cl <sub>2</sub>	SO <sub>2</sub>	Cl <sub>2</sub>	SO <sub>2</sub>
Zn-Cr-LDH	0.1	38	88	80	111
	0.5	19	62	111	130
	1	11	43	112	170
	10	10	36	117	205
	50	8	25	141	258
	100	5	20	146	271

### Resistance stabilization study

By consistently monitoring the pressure change of the photodiode as well as after introducing target gas at RT, we were able to learn about the energy playing ability of pure "Zn-Cr-LDH". The initial resistance stabilization curve of pure "Zn-Cr-LDH" is shown in Figure 7. Due to an increase in oxygen concentration on the Zn-Cr-surface, LDH's oxidising and reduction gases are adsorbed and undergo a heterogeneous catalytic process.



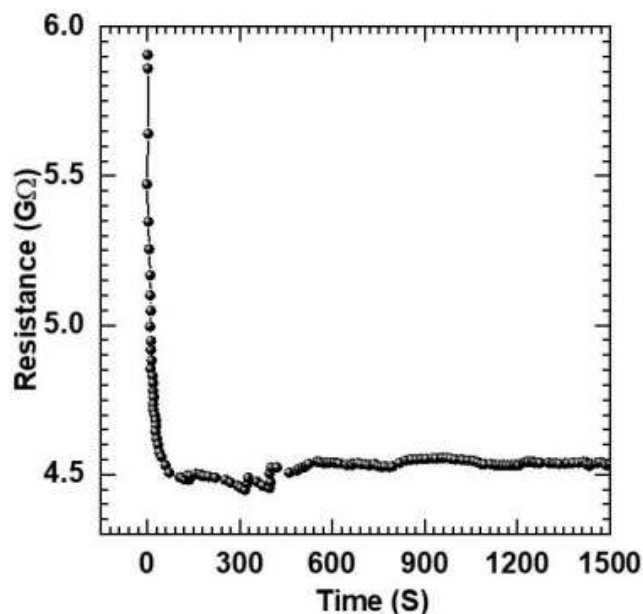
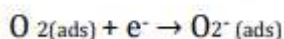
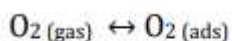


Figure 7. Initial stabilization curve of resistance of “Zn-Cr-LDH” at RT (27±2 °C).

In order to observe the gas's behaviour before introducing it to the "Zn-Cr-LDH," the opposition was performed three times for a total of 25 minutes. Adsorbed oxygen on "Zn-Cr-LDH" through the following stages before being exposed to gas, as represented by the eqs:



In Figure 7, we can see the resistivity of undiluted "Zn-Cr-LDH." it will rapidly decelerate from 7 to 4 G, then stabilise at 4.4 G.

### Selectivity study

Therefore, the selective response of a pure "Zn-Cr-LDH" sensor is vital to its potential for wide-ranging employment in a range of situations, since it dictates whether or not the responsive element can properly identify the target.

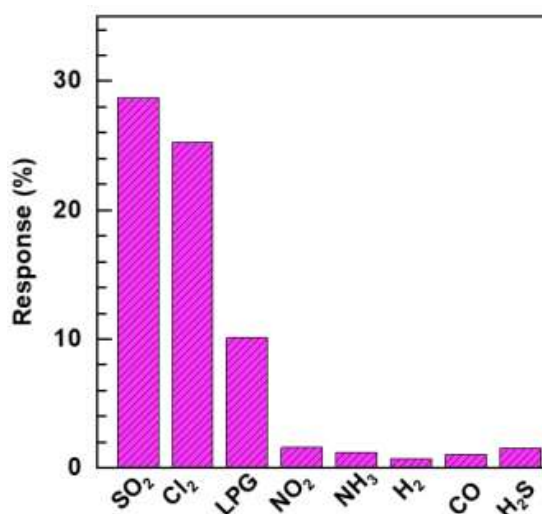


Figure 8. “The bar chart shows the response of “Zn-Cr-LDH” sensor for eight different target gases at RT (27±2 °C)”.

At ambient temperature, the activity of a pure “Zn-Cr-LDH” sensor system to 100 ppm of oxidising (NO<sub>2</sub>, NH<sub>3</sub>, CO, H<sub>2</sub>S) gases was detected. Magnificent Zn-Cr-related LDH's responses to a range of as a bar diagram in Figure 8. Ideal "Zn-Cr LDH" sensors respond differently to Cl<sub>2</sub> and SO<sub>2</sub> when isolated from other test gases at RT. Consequently, this is the only spot where you may use your Cl<sub>2</sub> and SO<sub>2</sub> gas detection credits.

### Response and resistance vs time transient study

For instance, in Figure 9 we find that the impedance vs. time behaviour sensitivity of pure "Zn Cr-LDH" is evaluated when subjected to 100 ppm Cl<sub>2</sub> and SO<sub>2</sub> at RT (27<sup>o</sup>C) (a, b). The resistance of pure Zn Cr-LDH quickly reduces when it is exposed to Cl<sub>2</sub> and SO<sub>2</sub> gas.

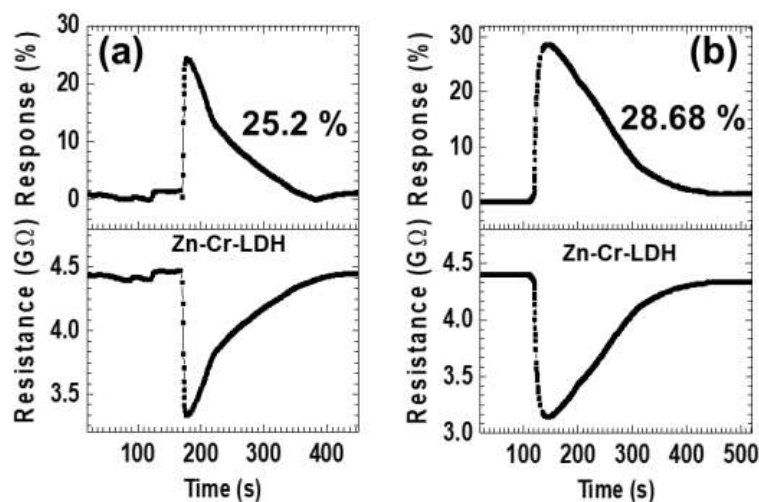


Figure 9. “Response and resistance vs time transients of “Zn-Cr-LDH” for 100 ppm (a) Cl<sub>2</sub> and (b) SO<sub>2</sub>.”

Because oxidizers like Cl<sub>2</sub> and SO<sub>2</sub> gas induce surface electrons to be acquired via vaporous iotas, they play a notable role in determining the functional reduction. Furthermore, low check numbers on the gas sensor's outer layer's sensitivity to Cl<sub>2</sub> and SO<sub>2</sub> suggest a P-type semiconducting technique to managing the behaviour of perfect "Zn-Cr-LDH." At 100 parts per million, Cl<sub>2</sub> and SO<sub>2</sub> gas are respectively 25.2% and 28.68% of the dazzling "Zn-Cr-LDH" gas.

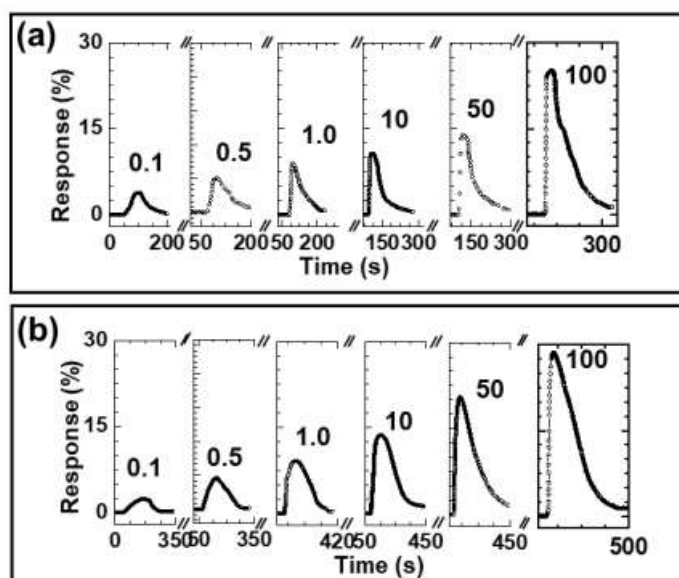


Figure 10. “Dynamic response curves of “Zn-Cr-LDH” sensor exposed to different Cl<sub>2</sub> and SO<sub>2</sub> concentrations (0.1, 0.5, 1, 10, 50, and 100 ppm)”.

The "Zn-Cr-LDH" sensor is sensitive to a broad range of Cl<sub>2</sub> and SO<sub>2</sub> concentrations with no change in impedance, and displays quick responsiveness upon target analyte presentation as well as amazing recovery of individuals with a sensation upon fuel removal at RT. The extraordinary "Zn-Cr-LDH" loses credibility when Cl<sub>2</sub> gas levels in the atmosphere climb from 2% to 25.2%. (0.1-100 ppm). Rates (percent) of ideal "Zn-Cr-LDH" reactions were 2, 5.2, 9, 11.5, 14, and 25.2% among groups exposed to 0.1, 0.5, 1, 10, 50, and 100 ppm of Cl<sub>2</sub>. Similarly, an increase in SO<sub>2</sub> concentration causes an increase in the effective sensitivity of unanticipated "Zn-Cr-LDH," from 2.27 to 28.68%. (0.1-100 ppm). Sheet-like architecture and limited layered growth in Zn-Cr-nonporous LDH are to account for its low perceived value when compared to the fantastic "Zn-Cr-LDH" for the target gases (Cl<sub>2</sub> and SO<sub>2</sub>). Pure "Zn-Cr-LDH" requires a technique that includes a lot of surface area, an airy design, and the best possible provided alliance in order to properly stimulate the care and selectivity of the enzyme.

## CONCLUSIONS

Prepared "Zn-Cr-LDH" in nitrate architecture was, in general, the result of an organized coprecipitation framework. Orthorhombic progress at the R-3 m stage was the concealed objective of the enquiry at the hexa LDH level. In this case, FT-IR and micro-Raman rotation were used to transmit the intercalation of nitrate anion in Zn-Cr LDH. Analysis of the surface morphology of Zn Cr-LDH showed that it was smooth, nonporous, and not refractory. The BET technique demonstrates that the clear surface area of "Zn-Cr-LDH" is rather tiny. The "Zn-Cr-LDH" was tested as a sensing material at room temperature (27.8 °C) using a well-designed gas sensor module. Both Cl<sub>2</sub> and SO<sub>2</sub> gases exhibited extraordinary organization of the ideal "Zn-Cr-LDH" when diverted from other target gases. The "Zn-Cr-LDH" was the most oversensitive of the bunch, reporting 25.2% at 100 ppm for Cl<sub>2</sub> and 28.68% for SO<sub>2</sub> gases. To similarly allow for contemplation and selection of perfect "Zn-Cr-LDH," the approach should have a big surface area, a more flexible game strategy, and an ideal conveyed synthesis.

## REFERENCES

1. Wongrat E, Hongsith N, Wongratanaphisan D, et al. *Sens. Actuators B Chem.* 2012; 172: 230-7p.
2. Wang Q, Huang J, Zhou J, et al. *Sens. Actuators B Chem.* 2018; 275: 306-11p.
3. Ma J, Fan H, Tian H, et al. *Sens. Actuators B Chem.* 2018; 262: 17- 25p.
4. Zhou Q, Zeng W, Chen W, et al. *Sens. Actuators B Chem.* 2019; 298: 126870p.
5. Liu L, Liu S. *ACS Sustainable Chem. Eng.* 2018; 10: 13427-34p.
6. Yang Z, Zhu, Jing J, et al. A review on strategies to LDH-based materials to improve adsorption capacity and photoreduction efficiency for CO<sub>2</sub>. *Coordination Chemistry Reviews.* 2019; 386: 154–82p.
7. Li T, Miras HN, Song YF. Polyoxometalate (POM)-Layered Double Hydroxides (LDH) composite materials: Design and catalytic applications. *Catalysts.* 2017; 7: 7–10p.
8. Zhu H, Balaban AT, Klein DJ, et al. Zivkovic, Co Co Co Co Co Co. *Scientific Reports.* 1994; 1675: 1–26p.
9. Li C, Wei M, Evans DG, et al. Layered double hydroxide-based nanomaterials as highly efficient catalysts and adsorbents. *Small.* 2014; 10: 4469–86p.